On–off intermittency: Power spectrum and fractal properties of time series

Shankar C. Venkataramani [a],*, Thomas M. Antonsen Jr. [a,1], Edward Ott [a,1,2], John C. Sommerer [b]

[a] *Institute for Plasma Research and Department of Physics, University of Maryland, College Park, MD 20742, USA*
[b] *M.S. Eisenhower Research Center, Johns Hopkins Applied Physics Laboratory, Laurel, MD 20723, USA*

Abstract

Some dynamical systems possess invariant submanifolds such that the dynamics restricted to the invariant submanifold is chaotic. This situation arises in systems with a spatial symmetry or in the synchronization of chaotic oscillators. The invariant submanifold could become unstable to perturbations in the transverse directions when a parameter of the system is changed through a critical *blow-out* value. This could result in an extreme form of temporally intermittent bursting called *on–off intermittency*.

We propose a model that incorporates the universal features of systems that display on–off intermittency. We study this model both with and without additive noise and we derive scaling results for the power spectral density of the on–off intermittent process and for the box counting dimension for the set of time intervals when the process takes on values above a given threshold. We then present numerical simulations realizing these results.

Keywords: On–off intermittency; Power spectrum; Fractal dimension; Universal scaling; Invariant manifold

1. Introduction

A recent paper [1], studied the consequences for a dynamical system of having an invariant manifold [3] on which the dynamics is chaotic, embedded in a phase space of larger dimensionality. This situation is illustrated schematically in Fig. 1.

It was further supposed that the invariant manifold has the property that on changing a parameter p of the system through a critical value p_c, the invariant manifold goes from being stable for $p < p_c$ (attracting on average for a set of initial conditions close to it) to being unstable for $p > p_c$ (repelling on average for a set of initial conditions close to it). This transformation has been called a *blow-out bifurcation* [1].

---

* Corresponding author.
[1] Also at Department of Electrical Engineering.
[2] Also at Institute for Systems Research.
[3] A manifold is invariant if for every initial condition in the manifold, the subsequent orbit remains in the manifold.
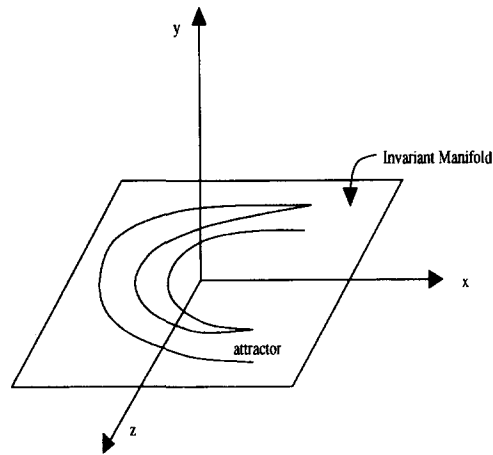
Fig. 1. A schematic of an invariant manifold with an embedded attractor. For initial conditions in the plane, the subsequent orbit remains in the plane.

The authors of Ref. [1] showed that, depending on the global dynamics in the phase space, there are two possibilities of particular interest:

(1) For p values near p_c with $p < p_c$, there is an attractor in the phase space that is not in the invariant manifold and the basin of the attractor in the invariant manifold is *riddled* by pieces of the basin of the attractor off the invariant manifold [1]. The basin of the attractor in the manifold is riddled in the sense that every point in it has points of the basin of the other attractor arbitrarily close to it.

(2) For $p < p_c$, the basin of the attractor in the invariant manifold is not riddled. [4] For p values near p_c with $p > p_c$, the system spends long periods of time in the vicinity of the invariant manifold. These intervals are interspersed with short bursts where the system moves away from the invariant manifold. This behavior is characteristic of an extreme form of temporally intermittent bursting called *on–off intermittency* [1,2].

Which of the two situations applies depends on the dynamics off the invariant manifold. This paper is restricted to a discussion of the second of the above possibilities. In particular, we study the dynamics of systems displaying on–off intermittency and look at possible signatures of this kind of behavior.

This paper is organized as follows. In Section 2, we discuss some physical situations that could display on–off intermittency. In Section 3, we summarize our results and compare our results with those reported in the literature [2–19]. We also present numerical evidence that supports our results. In Section 4 we propose a continuous-time model that displays on–off intermittency and incorporates the effects of additive noise. In Section 5, we study this model in the limit of no noise. In Section 6, we look at the effect of additive noise on the continuous-time model. In Section 7 we introduce a discrete-time version of the model in Section 4. We show that the discrete-time model is equivalent to sampling the continuous-time model and we then numerically verify our results by simulations of this model.

2. Systems with invariant manifolds

Systems with chaotic dynamics on an invariant manifold of smaller dimension than that of the entire phase space occur in many contexts. One class of situations where invariant manifolds arise naturally is in the synchronization

---

[4] Note that this does not imply that there are no other attractors in the phase space.
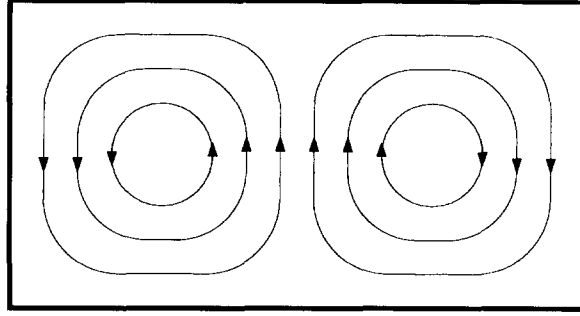
Fig. 2. Schematic illustration of a Rayleigh–Bernard cell with two symmetric rolls.

of identical chaotic oscillators [3]. For the case of two oscillators, the synchronized state is an invariant manifold of dimension equal to half that of the phase space. Another class of examples is physical systems with a spatial symmetry. An example is a Rayleigh–Bernard cell that is symmetric about its mid-plane. In such a cell, it is possible to setup a flow with two rolls symmetric about the mid-plane as in Fig. 2. Assume that the conditions (e.g. parameter values) are such that the time-dependence of these rolls is chaotic, while the velocity of the fluid is symmetric about the mid-plane for each instant of time. This symmetric motion represents motion in an invariant plane in the entire phase space. For example, the phase space can be represented by the set of coefficients in a Fourier expansion of the velocity field. Then, the invariant plane is specified by setting all the coefficients of the modes that represent asymmetric motion to zero. This situation could undergo a blow-out bifurcation to on–off intermittency if we change a parameter of the system. Then, we would see nearly spatially symmetric motion for long periods of time interspersed with short bursts of spatially asymmetric motion.

Rayleigh–Bernard experiments along these lines appear to be feasible (L. Howe and R. Behringer, private communication). Also, we note that experiments observing on–off intermittency in synchronized electric circuits have been performed [3,4].

An example of a system with spatial symmetry that has been studied in the literature is the two-dimensional motion in the XY-plane of a particle of unit mass in the potential [1]

$$V(X, Y) = (1 - X^2)^2 + Y^2(X - p) + KY^4, \tag{1}$$

with a sinusoidal forcing in time along the X-direction, and having a coefficient of friction ν. The quantity p in (1) will serve as the bifurcation parameter in what follows. The equations of motion are:

$$\begin{aligned}
\frac{dX}{dt} &= V_X, \\
\frac{dV_X}{dt} &= -\nu V_X + 4X(1 - X^2) + Y^2 + f_0 \sin(\omega t), \\
\frac{dY}{dt} &= V_Y, \\
\frac{dV_Y}{dt} &= -\nu V_Y - 2Y(X - p) - 4KY^3,
\end{aligned} \tag{2}$$

where f_0 and ω are the amplitude and the frequency of the sinusoidal forcing.

The full phase space is five-dimensional with coordinates X, Y, V_X, V_Y and $\theta = \omega t \bmod 2\pi$. Because of the reflection symmetry of the potential about $Y = 0$, we have that $Y = V_Y = 0$ is an invariant manifold for the dynamical system Eqs. (2). The motion in the invariant manifold is governed by the equation
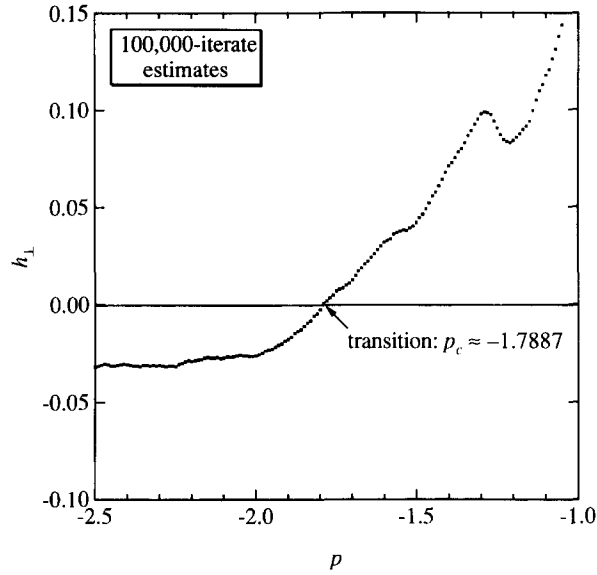
Fig. 3. $h_\perp$ as a function of p for the system in Eqs. (2) with $\nu = 0.05$, $f_0 = 2.3$ and $\omega = 3.5$. This plot was obtained by the authors of [1].

$$\frac{d^2 X}{dt^2} + \nu \frac{dX}{dt} + 4X(1 - X^2) = f_0 \sin(\omega t), \tag{3}$$

which is obtained by setting $Y = V_Y = 0$ in Eqs. (2). The system (3), with the parameters $\nu = 0.05$, $f_0 = 2.3$ and $\omega = 3.5$ has been studied by the authors of Ref. [1]. They show that, with these parameters, Eq. (3) has a chaotic attractor for the dynamics restricted to the invariant manifold.

The evolution of infinitesimal perturbations $(\delta Y, \delta V_Y)$ transverse to the invariant manifold is obtained by varying the system of equations in (2) about $Y = 0$. This yields

$$\frac{d\delta Y}{dt} = \delta V_Y,$$

$$\frac{d\delta V_Y}{dt} = -\nu \delta V_Y - 2\delta Y(X(t) - p), \tag{4}$$

where $X(t)$ represnts the solution to Eq. (3).

Let

$$\delta(t) = \sqrt{(\delta Y(t))^2 + (\delta V_Y(t))^2} \tag{5}$$

represent the infinitesimal distance from the invariant manifold.

We define the transverse Lyapunov exponent $h_\perp$ by

$$h_\perp = \lim_{t \to \infty} \frac{1}{t} \log(\delta(t)). \tag{6}$$

The limit has the same value for almost every choice of initial condition $(X(0), V_X(0), \theta(0))$ on the chaotic attractor and almost every choice of the orientation of the initial vector $(\delta Y(0), \delta V_Y(0))$.

A plot of $h_\perp$ vs. p for the parameters considered in [1] is shown in Fig. 3. As p is increased through the critical blow-out value $p_c = -1.7887$, the invariant manifold becomes unstable on average in the transverse direction (i.e., $h_\perp > 0$).
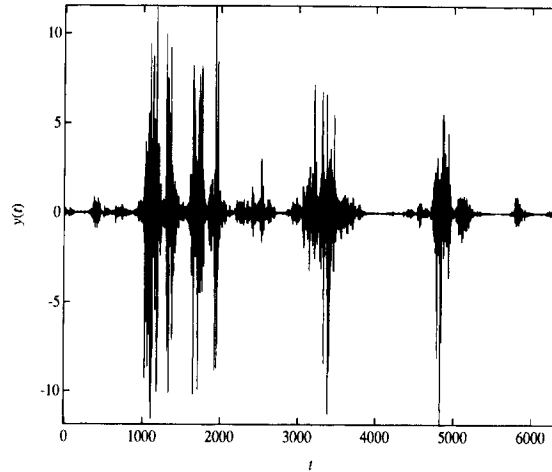
Fig. 4. Time series for the on–off intermittent process. This is a plot of $Y(t)$ obtained by numerically integrating the system of equations in (2) with $\nu = 0.05$, $f_0 = 2.3$, $\omega = 3.5$ and $p = -1.78 > p_c$.

We define the finite-time transverse Lyapunov exponents by

$$\tilde{h}_\perp(t) = \max_{\hat{n}} \left(\frac{1}{t} \log \left(\frac{\delta(t)}{\delta(0)} \right) \right), \tag{7}$$

where $\hat{n}$ is a unit vector along the direction of the initial displacement transverse to the invariant manifold. The finite-time Lyapunov exponents depend on the initial conditions $(X(0), V_X(0), \theta(0))$ on the chaotic attractor embedded in the invariant manifold. To characterize the variations in $\tilde{h}_\perp(t)$, we define the quantity D by

$$D = \frac{1}{2} \lim_{t \to \infty} t \left[E[(\tilde{h}_\perp(t))^2] - (E[\tilde{h}_\perp(t)])^2 \right], \tag{8}$$

where the expectation (denoted by E) is over all initial conditions $(X(0), V_X(0), \theta(0))$ according to the *natural measure* (here the natural measure is the measure produced by almost all initial conditions with respect to the Lebesgue measure in the chaotic attractor's basin restricted to the invariant manifold) on the chaotic attractor. We assume the limit in (8) exists.

For the system to display on–off intermittency, we require that $h_\perp$ be slightly larger than zero and that D not equal to zero. In this case, even if the system starts out near the invariant manifold it will (typically) eventually move away since the average Lyapunov exponent transverse to the invariant manifold is positive. We also need that there be fluctuations in the transverse finite time Lyapunov exponents ($D > 0$), such that there are periods of time when the transverse finite-time Lyapunov exponent is negative.[5] As we shall see this will cause the system to spend long stretches of time near the invariant manifold although the invariant manifold is repelling on average.

The authors of Ref. [1] argue that if the strength K of the quartic term in the potential (Eq. (1)) is sufficiently large, the confining effect of the KY^4 potential term will eliminate the possibility of attractors[6] off the invariant manifold. As there is only one attractor in the system for $p < p_c$, the system will display on–off intermittency when p is slightly larger than p_c. Fig. 4 shows a time series for $Y(t)$ that is obtained by numerically integrating the system of equations in (2) with $K = 0.0075$. Note that $Y(t)$ is close to the invariant manifold $Y = 0$ for

---

[5] Only very special systems would be expected to have $D = 0$.

[6] The authors of [1] show that there exists a pair of symmetrically disposed attractors off the invariant manifold for a smaller value of K.

long periods of time which are interspersed with bursts where $Y(t)$ moves away from the invariant manifold $Y = 0$.

In this system, a small amount of additive noise will destroy the invariant manifold in the sense that a unit mass starting out with $Y = V_Y = 0$ will no longer remain in the manifold $Y = V_Y = 0$. As we expect physical systems to have additive noise, we study the effect of noise on on–off intermittency (Sections 6 and 7).

The system of equations in (2) has the special property that the equation of motion in the invariant manifold, Eq. (3), is independent of the bifurcation parameter p.[7] We do not expect that this will always be the case. In a system without this property, we can still define a blow-out bifurcation if there is a critical value p_c of the bifurcation parameter p such that $h_\perp = 0$ at $p = p_c$ and the system has a chaotic attractor in the invariant manifold. As the attractor in the invariant manifold can itself undergo bifurcations as we change p, the quantities $h_\perp$ and D are not necessarily smooth or even continuous functions of p in the vicinity of p_c. However, we expect that, in a general system, the functions $h_\perp(p)$ and $D(p)$ will have smooth envelopes. In this case, our scaling results (reported in subsequent sections) should hold with respect to the smooth envelopes for these functions. The expectation that $h_\perp(p)$ and $D(p)$ have smooth envelopes is based on similar behavior observed in other cases. For example, if one plots the Lyapunov exponent h for the logistic map as a function of the parameter for parameter values between the period doubling accumulation point and the final crisis, one observes that h abruptly drops to negative values in parameter intervals where the attractor becomes periodic, but the overall appearance of an h versus parameter plot is that of a regular gradual increase with parameter that has a smooth upper bounding envelope.

3. Results

In the following, we study an on–off intermittent processes, both with and without additive noise. We show the following:

(i) The power spectrum $\overline{P}(\omega)$ of an on–off intermittent process with no noise scales as

$$\overline{P}(\omega) \sim \frac{1}{\sqrt{\omega}} \tag{9}$$

over a range of frequencies

$$\frac{h_\perp^2}{D} \ll \omega \ll D. \tag{10}$$

This is illustrated in Fig. 5 which shows a numerically obtained power spectrum of the process $|Y(t)|$ obtained by numerically integrating the system of equations in (2).

(ii) The level sets $Y = Y_0$, approach a Cantor set of dimension $\frac{1}{2}$ as $h_\perp \to 0^+$ (i.e., $p \to p_c$ from above). In particular, say we draw a horizontal line at $Y = 1$ in Fig. 4. We determine the scaled time coordinate $\tau = h_\perp^2 t / D$ at the intersections of $Y(t)$ with the horizontal line. We examine the values of the points of intersection in a range $0 \le \tau \le 1$. We divide this interval into equal subintervals of length ϵ. Let $N(\epsilon)$ denote the number of these subintervals that contain points where $Y(t)$ intersects the horizontal line. Then, for small positive $h_\perp$ (i.e., p near p_c), $N(\epsilon)$ scales with ϵ as

$$N(\epsilon) \sim \epsilon^{-1/2} \tag{11}$$

---

[7] Ashwin et al. [5] call such parameters *normal parameters*. Changing p does not affect the ergodic invariant measures of the dynamical system whose support is contained in the invariant manifold. Normal parameters arise naturally in the context of synchronization of identical chaotic oscillators.
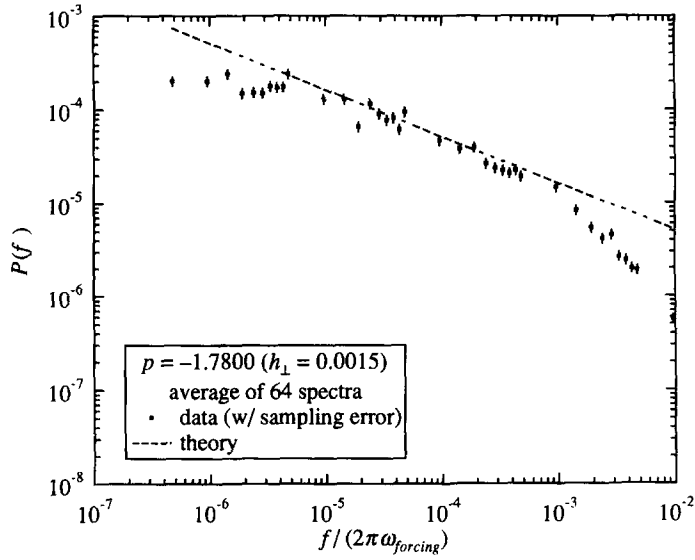
Fig. 5. The power spectral density for the process $|Y(t)|$ in the system of equations (2). Both the axes are on log-scales.
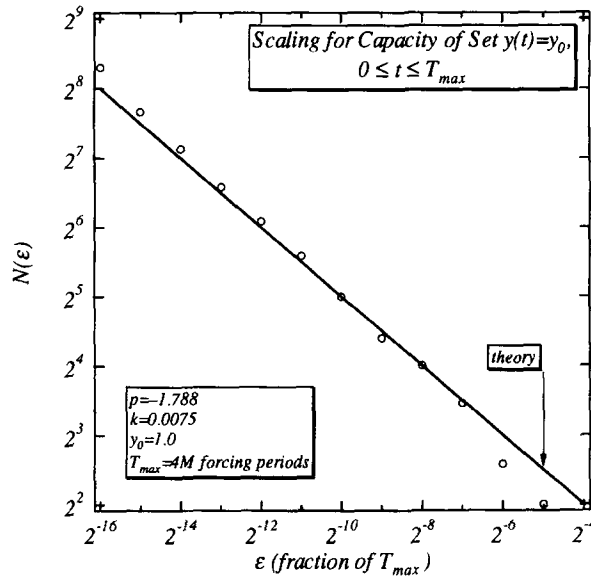
Fig. 6. Scaling of the number of boxes with ϵ.

for ϵ in a range

$$\frac{h_\perp^2}{D^2} \ll \epsilon \ll 1. \tag{12}$$

Fig. 6. shows a plot of $N(\epsilon)$ as a function of ϵ obtained by numerically integrating the system of equations in (2). Similarly, let $N_1(\epsilon)$ denote the number of subintervals of length ϵ that contain points where $Y(t) \geq Y_0$. Then, $N_1(\epsilon)$ also scales with ϵ as in (11) and (12).

(iii) In the presence of additive noise, the bursts when the system leaves the vicinity of the invariant manifold are more frequent. As a result, the range of frequencies where $\overline{P}(\omega) \sim 1/\sqrt{\omega}$ is smaller than in the case without noise,

$$\max \left(D \left[\log \left(\frac{D}{\sigma^2} \right) \right]^{-2}, \frac{h_\perp^2}{D} \right) \ll \omega \ll D, \tag{13}$$

where σ^2 is the noise power normalized by the amplitude of a typical burst. With noise, $N(\epsilon)$ again scales as $\epsilon^{-1/2}$ but now for ϵ in the range

$$\frac{h_\perp^2}{D^2} \ll \epsilon \ll \min \left(\frac{h_\perp^2}{D^2} \left[\log \left(\frac{D}{\sigma^2} \right) \right]^2, 1 \right). \tag{14}$$

Various mechanisms for intermittency have been studied in the literature. Pomeau and Manneville [17] study intermittency caused by a periodic orbit becoming unstable. This should be compared with on–off intermittency where the onset of intermittency occurs when a chaotic attractor (rather than a periodic orbit) loses stability.

A mechanism for intermittency in systems with symmetry is the intermittency caused by small random (additive noise) or periodic perturbations in systems that possess homoclinic orbits that are attracting. This mechanism has been studied by Stone and Holmes [18,19]. They show that the distribution of laminar phases has an exponential tail. This kind of intermittency is driven by the noise or periodic perturbations unlike on–off intermittency. Also, the distribution of laminar phases has an exponential tail unlike in on–off intermittency where the distribution of laminar phases has a power-law tail [14].

On–off intermittency has been studied by various authors [2–16]. Fujisaka et al. [6] looked at the power spectrum of an on–off intermittent time series without any additive noise. They predicted the noiseless scaling relation (9) for the power-spectrum. However, they were unable to observe this relation in their numerical simulations.

Heagy et al. [14] studied on–off intermittency in one-dimensional maps multiplicatively coupled to a driving signal that is either chaotic or random. They looked at the onset of intermittency, the scaling of the mean duration of a laminar phase (i.e., a time interval between bursts) and the distribution of the durations of laminar phases. As we will discuss later, the distribution of the duration of the laminar phases that these authors obtained is consistent with our result (ii) that the level sets approach a Cantor set with a dimension $D_0 = \frac{1}{2}$. Platt et al. [15] looked at the effect of additive noise on these quantities using an *elastic barrier* approximation. The elastic barrier approximation consists of treating the effect of noise by placing an impenetrable barrier at the noise level.[8] We do not make this approximation. Our result (14) is consistent with the location of the cutoff found using the elastic barrier approximation [15], and we also obtain the precise functional form of the cutoff (Eq. (A.74) and Fig. 11). This form is expected to be universal, and therefore may be testable in experiments.

4. Continuous-time model

Let $(u_1, u_2, \ldots, u_m, v_1, \ldots, v_{n-m})$ be coordinates on the phase space of an n-dimensional system with an invariant manifold $v_1 = v_2 = \cdots = v_{n-m} = 0$.[9] The dynamics depends on a parameter p whose value is such that the dynamics in the invariant manifold is chaotic. The system evolves as

---

[8] This approach has been used in [20] to study the effect of noise on the transient time that a system spends near an invariant manifold in the riddled basin case.

[9] One cannot always find coordinates globally on phase space such that the invariant manifold has this special form. We assume this as it makes our arguments easier to state. Our conclusions are valid even if we cannot find coordinates with the property that $v_1 = v_2 = \cdots = v_{n-m} = 0$ is an invariant manifold.

$$u_i(t) = u_i(u_1(0), \ldots, u_m(0), v_1(0), \ldots, v_{n-m}(0), t, p), \quad 1 \leq i \leq m,$$

$$v_i(t) = v_i(u_1(0), \ldots, u_m(0), v_1(0), \ldots, v_{n-m}(0), t, p), \quad 1 \leq i \leq n - m, \tag{15}$$

where $(u_1(0), \ldots, u_m(0), v_1(0), \ldots, v_{n-m}(0))$ are the values of the initial conditions. Since $v_1 = v_2 = \cdots = v_{n-m} = 0$ is an invariant manifold, we have

$$v_i(u_1(0), \ldots, u_m(0), 0, \ldots, 0, t, p) = 0 \quad \text{for all } t \text{ and } 1 \leq i \leq n - m. \tag{16}$$

Linearizing the equations in (15) for initial conditions close to the invariant manifold, we have

$$\delta v_i(t) \approx \sum_j M(t)_{ij} \delta v_j(0), \tag{17}$$

where $M(t)$ is a $(n - m) \times (n - m)$ matrix defined by

$$M(t)_{ij} = \frac{\partial}{\partial v_j(0)} v_i(u_1(0), \ldots, u_m(0), v_1(0), \ldots, v_{n-m}(0))\Big|_{v_1(0)=\cdots=v_{n-m}(0)=0}. \tag{18}$$

The matrix $M(t)$ depends on the initial conditions $(u_1, \ldots, u_m)$ in the invariant manifold and the value of the parameter p. We assume that there is a critical value p_c such that for $p < p_c$, the invariant manifold is stable on average in the sense that the transverse Lyapunov numbers given by the eigenvalues of the matrix

$$Q = \lim_{t \to \infty} [M^T(t)M(t)]^{1/2t} \tag{19}$$

are all less than unity. Oseledec's multiplicative ergodic theorem [21,22] guarantees the existence of the limit in (19).

For $p > p_c$ with $p - p_c$ sufficiently small, we assume that one of the eigenvalues of Q exceeds 1 slightly, while the other eigenvalues are less than one. Under these conditions, it is reasonable to suppose that for not too small t, the eigenvalue of $M(t)$ with the largest modulus, denoted by $\lambda(t)$ (If a pair of complex conjugate eigenvalues have moduli greater than one, we can choose either of them.), is such that $|\lambda(t)|^{1/t}$ has a modulus that fluctuates about 1 and all the other eigenvalues have a moduli whose tth root is less than one.

Ashwin et al. [5] show that this argument can be made rigorous. If we assume that p is a normal parameter for the dynamical system and the chaotic attractor in the invariant manifold is a Sinai–Bowen–Ruelle (SBR) attractor, then p_c is the critical value where the largest normal Lyapunov exponent for almost every initial condition is $\Lambda_{\text{SBR}} > 0$. Further, as p is a normal parameter, $\Lambda_{\text{SBR}}(p)$ is a continuous function of p that goes through 0 as p goes through p_c. Therefore, for $p < p_c$, all the normal Lyapunov exponents are negative and consequently all the eigenvalues have moduli less than one. For $p > p_c$ with p close to p_c, only the largest Lyapunov exponent is positive and all the others are negative. Therefore, one of the eigenvalues fluctuates about 1 while all the other eigenvalues have moduli less than 1. If we look at the deviation $\delta(t)$ from the invariant manifold

$$\delta(t) = \sqrt{\sum_j (\delta v_j(t))^2}, \tag{20}$$

at sufficiently large time, we have

$$\delta(t) \approx |\lambda(t)| \delta(0). \tag{21}$$

$\lambda(t)$ is related to the transverse Lyapunov exponent $h_\perp$ by

$$h_\perp = \lim_{t \to \infty} \frac{1}{t} \log(|\lambda(t)|). \tag{22}$$

As discussed earlier, if $h_\perp$ is positive and has a sufficiently small value and if there are fluctuations in $\log(|\lambda|)$ (i.e., $D > 0$), $\delta(t)$ is an on–off intermittent process. Therefore, though the full phase space is n dimensional, the deviation from the invariant manifold can be modelled by the one-dimensional equation

$$\frac{\mathrm{d}\delta(t)}{\mathrm{d}t} = h(t)\delta(t), \tag{23}$$

where

$$h(t) = \frac{\mathrm{d}}{\mathrm{d}t} \log(|\lambda(t)|). \tag{24}$$

The quantity $h(t)$ has a positive time average but if this average is small enough, $h(t)$ varies chaotically from positive to negative values. From the above discussion, we expect Eq. (23) to be a good model close to the invariant manifold. We generalize this to model a continuous-time intermittent process $x(t)$ in the presence of additive noise by

$$\frac{\mathrm{d}x}{\mathrm{d}t} = (h_\perp + \beta n_1)x + \sigma n_2, \tag{25}$$

where $h_\perp$ is the transverse Lyapunov exponent, βn_1 is a zero mean chaotic process that simulates the fluctuations in the finite-time transverse Lyapunov exponent and σn_2 represents the effects of noise in the system. The quantity $(h_\perp + \beta n_1)$ in (25) is to be identified with the quantity $h(t)$ in (23).

The chaotic process n_1 has a characteristic time scale beyond which its autocorrelation is negligible. By making $h_\perp$ sufficiently small, the typical time between bursts can be made long compared to the autocorrelation time of the chaotic process n_1. Thus, for $h_\perp$ sufficiently small (i.e., $(p - p_c) > 0$ sufficiently small) we are concerned with time scales much longer than the autocorrelation time of n_1. In this case, we can approximate n_1 as white noise and we take it to have unit variance. The process n_2, which simulates the noise in the system can also be taken as unit variance white noise and is uncorrelated with n_1. Even if the noise n_2 had temporal correlations, for sufficiently small $h_\perp$ they can be neglected.

We expect that Eq. (23) should be modified for large $\delta(t)$ as Eq. (17) is only approximately true away from the invariant manifold. For a real system, there will be non-linear corrections to Eq. (23) that keep the motion bounded. These corrections will be important only when the system is far away from the inariant manifold. We incorporate the effect of these non-linearities in our model by having reflecting (no flux) boundary conditions at $x = 1$ and at $x = -1$. In the limit $h_\perp \to 0$, the system will remain in the vicinity of the invariant manifold most of the time and will burst away very infrequently. Therefore, the exact details of the non-linearities that keep the motion bounded are not important in determining the scaling dependence of the process, and the results that we derive for long time scales from our model with reflecting boundary conditions at $x = \pm 1$ are expected to be universal for small $h_\perp$. For small time scales, we can no longer approximate n_1 by white noise as the correlations in the chaotic process $h(t)$ in (23) become important. Let τ_c denote the correlation time of the chaotic process $h(t)$. We take $\tau_c \sim D^{-1}$. This is also the order of magnitude of the time it takes for the process to diffuse away from the boundaries i.e., for properties on this time scale, the exact details of the non-linearities that keep the motion bounded become important. Therefore, we expect that the scaling results we derive from our model are universal only in the frequency range $\omega \ll D$, i.e., for time scales τ such that

$$\tau \gg D^{-1}. \tag{26}$$

The transition probability density $p_*(x, t : x_0)$ is defined as the probability density of $x(t)$ having a value between x and $x + \mathrm{d}x$ given that $x(0) = x_0$. The transition probability density for the process in Eq. (25) satisfies the following Fokker–Planck (Forward Kolmogorov) equation (see Ref. [23] for details):

$$\frac{\partial p_*(x, t : x_0)}{\partial t} = \frac{1}{2} \frac{\partial^2}{\partial x^2} [b^2(x) p_*(x, t : x_0)] - \frac{\partial}{\partial x} [a(x) p_*(x, t : x_0)], \tag{27}$$

where the drift coefficient $a(x)$ and the diffusion coefficient $b(x)$ are given by

$$a(x) = \left(h_\perp + \frac{\beta^2}{2} \right) x,$$

$$b(x) = (\beta^2 x^2 + \sigma^2)^{1/2}. \tag{28}$$

If $\overline{p}_0(y)$ is the initial probability distribution, the probability distribution $p(x, t)$ at a time t is given by

$$p(x, t) = \int \mathrm{d}y \, p_*(x, t : y) \overline{p}_0(y). \tag{29}$$

Therefore, the probability distribution satisfies the forward equation

$$\frac{\partial p(x, t)}{\partial t} = \frac{1}{2} \frac{\partial^2}{\partial x^2} [b^2(x) p(x, t)] - \frac{\partial}{\partial x} [a(x) p(x, t)]. \tag{30}$$

The conservation of probability equation is given by

$$\frac{\partial p}{\partial t} + \frac{\partial \Gamma}{\partial x} = 0, \tag{31}$$

where Γ is the probability flux. Comparison with Eq. (30) yields

$$\Gamma(x, t) = -\frac{1}{2} (\beta^2 x^2 + \sigma^2) \frac{\partial p(x, t)}{\partial x} + \left(h_\perp - \frac{\beta^2}{2} \right) x p(x, t). \tag{32}$$

A reflecting boundary condition at $x = x_b$ is

$$\Gamma(x_b, t) = 0. \tag{33}$$

5. Noise-free model

In this section, we study the on–off intermittent process in Eq. (25) when there is no additive noise. We establish the results in Eqs. (9)–(12) of Section 3.

If there is no noise in the model, we can set $\sigma = 0$ in Eq. (28). If we start out at $t = t_0$ with $x_0 > 0$, then $x(t)$ is positive for all subsequent time t. Therefore, it is sufficient to consider x in the range [0,1]. It is convenient to introduce the variable $z = -\log(x)$. Expressing (30) and its associated boundary conditions in terms of the variable z gives the forward Kolmogorov equation for $p(z, t)$,

$$\frac{\partial p}{\partial t} = \frac{\beta^2}{2} \frac{\partial^2 p}{\partial z^2} + h_\perp \frac{\partial p}{\partial z}, \tag{34}$$

with the boundary conditions

$$p(z, t) \to 0 \quad \text{as } z \to \infty,$$

and

$$\left[\frac{\beta^2}{2} \frac{\partial p(z, t)}{\partial z} + h_\perp p(z, t) \right]_{z=0} = 0. \tag{35}$$

From the definition of the quantity D, Eq. (8), we see that for the model in Eq. (25) with n_1 being unit variance white noise, we have $D = \beta^2/2$. As the boundaries are reflecting, the total probability of finding x between 0 and 1 is unity independent of time. For long times the probability distribution of the variable z will tend to a steady state value $p_{ss}(z)$ which is determined by demanding that the flux vanish for all z. This implies,

$$D\frac{\partial p_{ss}(z)}{\partial z} + h_\perp p_{ss}(z) = 0. \tag{36}$$

We can solve (36) for the steady state probability distribution of z to obtain

$$p_{ss}(z) = \frac{h_\perp}{D} \exp\left(-\frac{h_\perp z}{D}\right). \tag{37}$$

5.1. Power spectral density

We consider the autocorrelation for the process $(x(t))^k$ where k is an arbitrary positive exponent. The autocorrelation is given by

$$R(\tau) = E[(x(t))^k (x(t+\tau))^k], \tag{38}$$

where $E[.]$ denotes the expectation over all realizations of the random process $x(t)$. Then,

$$R(\tau) = \int\limits_0^\infty dz\, p_{ss}(z)e^{-kz} \int\limits_0^\infty dz'\, p_*(z', \tau : z)e^{-kz'}, \tag{39}$$

where $p_*(z', t : z)$ is the transition probability density. Then, from Eq. (34), $p_*(z', t : z)$ satisfies the forward Kolmogorov equation

$$D\frac{\partial^2 p_*(z', t : z)}{\partial z'^2} + h_\perp \frac{\partial p_*(z', t : z)}{\partial z'} = \frac{\partial p_*(z', t : z)}{\partial t} \tag{40}$$

with the initial value condition

$$p_*(z', 0 : z) = \delta(z' - z),$$

and boundary conditions

$$p_*(z', t : z) \to 0 \quad \text{as } z' \to \infty,$$

and

$$\left[D\frac{\partial p_*(z', t : z)}{\partial z'} + h_\perp p_*(z', t : z)\right]_{z'=0} = 0$$

for all t. Let us define a new function $v(z', t)$ by

$$v(z', t) = \int\limits_0^\infty dz\, p_{ss}(z)e^{-kz} p_*(z', t : z). \tag{41}$$

Then, multiplying Eq. (40) by $p_{ss}(z)\exp(-kz)$ and integrating over z gives

$$D\frac{\partial^2 v(z', t)}{\partial z'^2} + h_\perp \frac{\partial v(z', t)}{\partial z'} = \frac{\partial v(z', t)}{\partial t} \tag{42}$$

with the initial condition

$$v(z', 0) = \frac{h_\perp}{D} \exp\left[-\left(\frac{h_\perp}{D} + k\right)z'\right], \tag{43}$$

and the same boundary conditions as $p_*(z', t : z)$. From Eq. (39) and the definition of $v(z', t)$, Eq. (41), the autocorrelation is given by

$$R(\tau) = \int_0^\infty v(z', \tau) e^{-kz'} \, dz'. \tag{44}$$

We next introduce the Laplace transform of the autocorrelation function by

$$\overline{R}(s) = \int_0^\infty R(t) e^{-st} \, dt. \tag{45}$$

Then, in terms of the function $v(z', t)$, we have that $\overline{R}(s)$ is given by

$$\overline{R}(s) = \int_0^\infty \overline{v}(z', s) e^{-kz'} \, dz', \tag{46}$$

where $\overline{v}(z', s)$ is the Laplace transform of $v(z', t)$. We obtain $\overline{v}(z', s)$ by taking the Laplace transform of Eq. (42) and solving the resulting ODE in z'. From this, we get

$$\overline{R}(s) = -\frac{1}{Dk^2 + h_\perp k - s} \left[\frac{h_\perp}{2kD + h_\perp} + \frac{4kD}{(1 - q)(2kD + h_\perp(1 + q))}\right], \tag{47}$$

where $q = \sqrt{1 + sT_0}$ and $T_0 = 4D/h_\perp^2$. Since $\lim_{\tau \to \infty} R(\tau) = (E[(x(t)^k])^2 \neq 0$, $\overline{R}(s)$ has a pole at $s = 0$ and the Fourier transform of the autocorrelation has a δ-function component at $\omega = 0$. To remove this delta function, we define the power spectral density $(psd) \overline{P}(\omega)$ as the Fourier transform of the autocovariance $P(\tau)$ which is given by

$$P(\tau) = E[(x(t))^k (x(t + \tau))^k] - (E[(x(t))^k])^2. \tag{48}$$

If $\overline{U}(s)$ is the Laplace transform of $P(t)$, we have

$$\overline{U}(s) = \overline{R}(s) - \frac{(E[(x(t))^k])^2}{s}, \tag{49}$$

and $\overline{U}(s)$ has no singularities in the right half s-plane or the imaginary axis. Therefore,

$$\overline{P}(\omega) = \overline{U}(i\omega) + \overline{U}(-i\omega) = \overline{R}(s = i\omega) + \overline{R}(s = -i\omega), \tag{50}$$

by Eq. (49). If we take the limit $h_\perp \to 0$ with $\omega \ll D$ in such a way that ωT_0 is finite, we get

$$\overline{P}(\omega) = \left(\frac{\sqrt{8}}{Dk^2}\right) \frac{\sqrt{(1 + (\omega T_0)^2)^{1/2} - 1}}{\omega T_0}. \tag{51}$$

Therefore, in the range $D \gg \omega \gg T_0^{-1} = h_\perp^2/4D$, we have

$$\overline{P}(\omega) \cong \frac{2}{Dk^2} \sqrt{\frac{2}{\omega T_0}}, \tag{52}$$

i.e., the power spectral density scales as $\omega^{-1/2}$ for $h_\perp^2/D \ll \omega \ll D$. Note that the scaling behavior and scaling range are independent of the index k.

As discussed in Section 4, for long time scales, i.e., for $\omega \ll D$, we expect that the scaling results obtained from our model are universal. The behavior of the process for these time scales is independent of the exact details of the chaotic process in the invariant manifold and the non-linearities that keep the process bounded. Therefore, we expect that Eqs. (51) and (52) will hold for all on–off intermittent processes without additive noise in the limit $h_\perp \to 0$. This demonstrates our results in item (i) of Section 3.

5.2. Fractal dimension

As we let $h_\perp \to 0^+$, the set of time intervals when the intermittent process takes on values above a given threshold approaches a fractal if we rescale time appropriately. We choose the threshold at $x = 1$ and rescale time by $\tau = h_\perp^2 t/D$. We look at the process in the range $0 \leq \tau \leq 1$. If the fractal dimension of the limiting set is d, the number of time intervals of length ϵ needed to cover the set scales as $N(\epsilon) \approx \epsilon^{-d}$. The total number of intervals of length ϵ in the interval $0 \leq \tau \leq 1$ is ϵ^{-1}. Therefore, the probability $P(\epsilon)$ that a randomly chosen interval of length ϵ is a part of the over of the limiting set is given by

$$P(\epsilon) \approx \frac{N(\epsilon)}{\epsilon^{-1}} \approx \epsilon^{1-d}. \tag{53}$$

Thus, we can calculate the fractal dimension d if we evaluate $P(\epsilon)$.

After a sufficiently large time t_m, the variable $z = -\log(x)$ is distributed according to the steady state distribution $p_{ss}(z)$ independent of the inital conditions. Then $P(\epsilon)$ is the probability that there exists some $t \in [t_m, t_m + D\epsilon/h_\perp^2]$ such that $x(t) \geq 1$. This is the same as the probability of being absorbed at $x = 1$ in an interval $0 \leq \tau \leq \epsilon$ if we start off with the steady state distribution and have absorbing boundary conditions at $x = 1$, i.e., at $z = 0$.

Therefore, we solve

$$\frac{\partial p(z,t)}{\partial t} = D \frac{\partial^2 p(z,t)}{\partial z^2} + h_\perp \frac{\partial p(z,t)}{\partial z} \tag{54}$$

with absorbing boundary conditions at $z = 0$

$$p(0,t) = 0 \quad \text{for all } t, \tag{55}$$

no flux as $z \to \infty$, i.e.,

$$p(z,t) \to 0 \quad \text{as } z \to \infty, \tag{56}$$

and the initial condition

$$p(z,0) = p_{ss}(z). \tag{57}$$

Let $W(t)$ be the probability of getting absorbed in the time interval from zero to (unscaled) time t. Then,

$$W(t) = 1 - \int_0^\infty p(z,t)\,dz. \tag{58}$$

Let us introduce $\overline{W}(s)$, the Laplace transform of $W(t)$. From Eq. (58) we obtain

$$\overline{W}(s) = \frac{1}{s} - \int_0^\infty \overline{p}(z, s)\, dz, \tag{59}$$

where $\overline{p}(z, s)$ is the Laplace transform of $p(z, t)$. Taking the Laplace transform of Eq. (54) and solving the resulting ODE with the appropriate boundary conditions, we obtain

$$\overline{p}(z, s) = \frac{h_\perp}{Ds} \left[\exp\left(-\frac{h_\perp z}{D}\right) - \exp\left(-\frac{\left(h_\perp + \sqrt{h_\perp^2 + 4Ds}\right)z}{2D}\right) \right]. \tag{60}$$

Thus,

$$\overline{W}(s) = \frac{2}{s(1 + \sqrt{1 + sT_0})}, \tag{61}$$

where $T_0 = 4D/h_\perp^2$ as defined in the previous section. For $sT_0 \gg 1$, i.e., time scales such that $t \ll T_0$,

$$\overline{W}(s) = \frac{2}{\sqrt{s^3 T_0}}. \tag{62}$$

Taking the inverse Laplace transform, we get

$$W(t) = 4\sqrt{\frac{t}{\pi T_0}} \tag{63}$$

for $t \ll T_0$. Therefore, $P(\epsilon) = W(D\epsilon / h_\perp^2)$ implies

$$P(\epsilon) \approx \epsilon^{1/2} \tag{64}$$

for $\epsilon \ll 1$. If $P(\epsilon) \approx \epsilon^x$, the fractal dimension $d = 1 - x$ by Eq. (53). Therefore, $d = 1/2$.

By Eq. (26), the results we derive from the model in (25) are universal only for $t \gg D^{-1}$, i.e., $\epsilon \gg h_\perp^2 / D^2$. Therefore, for a general on–off intermittent process, $N(\epsilon)$ scales as $\epsilon^{-1/2}$ for ϵ in the range $h_\perp^2 / D^2 \ll \epsilon \ll 1$. This demonstrates our results in item (ii) of Section 3.

The result we obtain that the fractal dimension of the limiting set is $D_0 = \frac{1}{2}$ is consistent with the results obtained by Heagy et al. [14] for the distribution of the length of the laminar phases. Let $N(\epsilon)$ be the number of intervals of length ϵ that are needed to cover the set of bursts. For $h_\perp^2 / D^2 \ll \epsilon \ll 1$, our results imply

$$N(2\epsilon) = \frac{N(\epsilon)}{\sqrt{2}}. \tag{65}$$

However,

$$N(2\epsilon) = N(\epsilon)(1 - b(\epsilon)), \tag{66}$$

where $b(\epsilon)$ is the probability that there is a peak in the interval $[(a + 1)\epsilon, (a + 2)\epsilon]$ given that there is a peak in $[a\epsilon, (a + 1)\epsilon]$. Every pair of such peaks will require two boxes in a cover by intervals of length ϵ but will only require one box in a cover by intervals of size 2ϵ. Comparing Eqs. (65) and (66) shows that, in the range of ϵ where $D_0 = 1/2$,

$$b(\epsilon) = 1 - \frac{1}{\sqrt{2}}. \tag{67}$$

Let $\Pi(\epsilon)$ denote the probability of having a laminar phase of a length greater than ϵ. Since $b(\epsilon)$ is the conditional probability that we have a laminar phase of length between ϵ and 2ϵ given that we have a laminar phase of length greater than ϵ, we obtain

$$b(\epsilon) = \frac{\Pi(\epsilon) - \Pi(2\epsilon)}{\Pi(\epsilon)}. \tag{68}$$

Eqs. (67) and (68) together yield

$$\frac{\Pi(2\epsilon)}{\Pi(\epsilon)} = \frac{1}{\sqrt{2}} \tag{69}$$

independent of ϵ in the range where $N(\epsilon) \sim \epsilon^{-1/2}$. Therefore,

$$\Pi(\epsilon) = \Pi_0 \epsilon^{-1/2}, \tag{70}$$

where Π_0 is a constant. If $\Lambda(\theta)$ is the probability density of having a laminar phase of (unscaled) length θ, we have

$$\Pi(\epsilon) = \int\limits_{D\epsilon/h_\perp^2}^{\infty} \Lambda(\theta)\, d\theta. \tag{71}$$

Using Eq. (70), we obtain

$$\Lambda(\theta) = \frac{\Pi_0 \sqrt{D}}{2h_\perp} \theta^{-3/2} \tag{72}$$

for $\theta \ll D/h_\perp^2$, which is consistent with the result obtained in [14].

6. On–off intermittency in noise

In this section we present analytic results derived from the continuous-time model in Eq. (25). The details of the calculations are spelt out in Appendix A. Eq. (25) models the deviation from the invariant manifold for an on–off intermittent process with a transverse Lyapunov exponent $h_\perp$, with $D = \beta^2/2$ in additive noise with power σ^2. We restrict the range of x by having no-flux boundary conditions at $x = \pm 1$.

As the process $x(t)$ takes on both positive and negative values we consider the power spectra of the processes x^{2k} with k integer. By the results for the noise free case where the scaling behavior was independent of the index k, we expect the results for the power spectrum will depend only weakly on k. In particular, we expect that the scaling exponent and range will be independent of k. Therefore, we only consider the case $k = 1$ in Appendix A. We define the autocorrelation $R(\tau)$ by

$$R(\tau) = E[x^2(t)x^2(t + \tau)], \tag{73}$$

where $E[.]$ denotes the expectation over all realizations of the process $x(t)$. In Appendix A, we derive an expression for $\overline{R}(s)$, the Laplace transform of the autocorrelation $R(\tau)$ which is given by Eqs. (A.18) and (A.36). From this, we obtain an expression for the power spectrum $\overline{P}(\omega)$ and derive the scaling relation

$$\overline{P}(\omega) \sim 1/\sqrt{\omega} \tag{74}$$

for

$$D > \omega > \omega_c, \tag{75}$$

where the cutoff frequency ω_c is given by

$$\omega_c = \max\left(\frac{h_\perp^2}{D}, 2\beta^2\left[\log\left(\frac{\beta^2}{\sigma^2}\right)\right]^{-2}\right) \tag{76}$$

as we show in Appendix A. This is the first part of our results in item (iii) of Section 3.

We can also determine the fractal dimension of the set of time intervals when the on-off intermittent process crosses a threshold. As we argue in Section 5.2, we need to calculate the probability $P(\epsilon)$ that a randomly chosen interval of rescaled length ϵ is a part of the cover of the set of times when the process takes on values on or above the given threshold. We choose the threshold at $|x| = 1$. As we discuss in Section 5.2, this probability is the same as the probability of getting absorbed at $x = \pm 1$ in an interval of length $D\epsilon/h_\perp^2$ if we start out in the steady state. We evaluate this probability in Appendix A (see Eq. (A.81)) to obtain

$$P(\epsilon) \sim \epsilon^{1/2} \tag{77}$$

for

$$h_\perp^2/D^2 \ll \epsilon \ll h_\perp^2/D\omega_c, \tag{78}$$

where ω_c is given by Eq. (76). By the discussion in Section 5.2 (Eq. (53)), $N(\epsilon) \sim \epsilon^{1/2}$ for $h_\perp^2/D^2 \ll \epsilon \ll h_\perp^2/D\omega_c$ which is the second part of our result in item (iii) of Section 3.

The discussion in Section 5.2 also implies that the distribution of the lengths of the laminar phases in noise is given by $\Lambda(\theta) \sim \theta^{-3/2}$ for $\theta \ll \omega_c^{-1}$. This is consistent with the results obtained in [15].

7. Discrete-time model

In this section, we introduce a discrete-time model that displays on–off intermittency and incorporates the effects of additive noise. Our motivation for looking at this discrete-time model is that it is particularly convenient for numerical simulations. We simulate this model numerically and we present the results of these simulations.

A straightforward way to generalize Eq. (23) to discrete-time systems is by [14]

$$y_{n+1} = e^{h_n} y_n \quad \text{for small } y_n, \tag{79}$$

where h_n is a chaotic process.

Using this approach, we model a discrete-time intermittent process restricted to $[-1,1]$ and with additive noise by

$$x_{n+1} = \begin{cases} \lambda_n x_n + \epsilon_n & \text{if } \lambda_n x_n + \epsilon_n \in [-1, 1], \\ x_n & \text{otherwise,} \end{cases} \tag{80}$$

where λ_n is generated by a discrete-time chaotic process and ϵ_n models the additive noise in the system. As discussed in Section 4, the behavior of the process at large time scales is independent of the details of how the processes λ_n and ϵ_n are generated. In the limit $h_\perp \to 0$, we are interested in time scales much longer than the correlation time of the chaotic process λ_n. Therefore, we can choose λ_n to be any random process such that, if $h_n = \log(\lambda_n)$, then

(1) h_n has a small positive mean.

(2) h_n has non-zero variations about its mean so that it is sometimes negative.

To satisfy these requirements, we generate the process λ_n by

$$\lambda_n = \begin{cases} \Delta^{-1} & \text{with probability } \alpha, \\ \Delta & \text{with probability } \gamma, \end{cases} \tag{81}$$

where $\Delta > 1$ and $\gamma = 1 - \alpha > \alpha$. Let $\bar{h} = E[h_n]$. Then,

$$\bar{h} = (\gamma - \alpha)K, \tag{82}$$

where $K = \log \Delta$. We have a blow-out bifurcation when $\bar{h}$ changes from a negative to a positive value, i.e., when $\alpha = \gamma = \frac{1}{2}$.

The process ϵ_n models the additive noise in the system. We choose ϵ_n to be a sequence of independent identically distributed (i.i.d) random variables that take on values $\pm\rho$ with probability $\frac{1}{2}$.

Consider the process x_n generated by sampling the continuous-time process in (25) with a period T_0. Then the discrete-time process x_n is given by $x_n = x(nT_0)$. If we set $\sigma = 0$ in (25), we have

$$E\left[\log\left(\frac{x((n+1)T_0)}{x(nT_0)}\right)\right] = h_\perp T_0,$$

$$E\left[\left(\log\left(\frac{x((n+1)T_0)}{x(nT_0)}\right) - h_\perp T_0\right)^2\right] = \beta^2 T_0. \tag{83}$$

If we set $\beta = 0$ in (25), for $mT_0 \ll h_\perp^{-1}$ and $m \gg 1$ we obtain

$$E[(x((n+m)T_0) - e^{mh_\perp T_0}x(nT_0))^2] = m\sigma^2 T_0. \tag{84}$$

Comparing Eqs. (83) and (84) with the model in (80), we see that the process x_n in (80) models a sampled continuous-time intermittent process if we make the identifications

$$\bar{h} = h_\perp T_0,$$
$$\log^2(\Delta) \approx 4\alpha\gamma K^2 = \beta^2 T_0,$$
$$\rho^2 = \sigma^2 T_0. \tag{85}$$

We define the autocorrelation of the discrete-time process x_n by

$$r_n = E[x_p x_{n+p}]. \tag{86}$$

Then, $r_n = R(nT_0)$ where $R(\tau)$ is defined in (38).

The autocovariance of the process x_n is defined by

$$p_n = r_n - (E[x_n])^2, \tag{87}$$

and the discrete-time Power Spectral Density $\tilde{P}(e^{i\omega})$, is the Discrete Fourier transform of the autocovariance. Therefore,

$$\tilde{P}(e^{i\omega}) = \sum_{n=-\infty}^{\infty} p_n e^{-in\omega}. \tag{88}$$

If T_0 is much smaller than the relevant timescales, the continuous-time process $x(t)$ is essentially a low-pass signal. By the Nyquist Sampling theorem [25], we obtain

$$\tilde{P}(e^{i\omega}) = \frac{1}{T_0}\bar{P}\left(\frac{\omega}{T_0}\right) \tag{89}$$

for $\omega \ll \pi$ where we can neglect the effects of aliasing. Using the identifications in (85) and Eq. (89), we can translate the results in Section 3 for the continuous-time model to the corresponding results for the discrete-time case. We obtain the following points.

(1) For a discrete-time on–off intermittent process without noise we have:

   (a) The power spectral density scales according to $\tilde{P}(e^{i\omega}) \sim 1\sqrt{\omega}$ for over the range $(\gamma - \alpha)^2 \ll \omega \ll \min(K^2, 1)$.

   (b) Let $\mathcal{N}$ denote the set of discrete-time indices n such that x_n is larger than or equal to a threshold a. We determine a scaled time coordinate $\tau = (\gamma - \alpha)^2 n$ and examine the set of these values in the limit $\bar{h} \to 0$. Then, the set of rescaled time indices when the process x_n is above a given threshold approaches a Cantor set. The Cantor set has a box counting dimension $D_0 = \frac{1}{2}$. If $N(\epsilon)$ is the number of boxes of length ϵ required to cover the set of rescaled time indices where $x_n \geq a$, we have the scaling result $N(\epsilon) \sim \epsilon^{-1/2}$ for $(\gamma - \alpha)^2 \ll \epsilon \ll 1$.

(2) In the presence of additive noise, the power spectrum scales as $1/\sqrt{\omega}$ in the range $\max(K^2/\log^2(K^2/\rho^2), (\gamma - \alpha)^2) \ll \omega \ll \min(K^2, 1)$ and $N(\epsilon)$ scales as $\epsilon^{-1/2}$ in the range $(\gamma - \alpha)^2 \ll \epsilon \leq \min((\gamma - \alpha)^2 \log^2(K^2/\rho^2), 1)$.

The results in items 1(a) and 1(b) can be verified analytically. [10] For the continuous-time power spectrum, the upper cutoff ω_u is D and the identifications in (85) imply that the upper cutoff for the discrete-time model should be K^2. However, the cutoff for the power spectrum obtained by a FFT could be lower because of the effects of aliasing [25] and the fact that we need the approximation

$$e^{i\omega} - 1 \approx i\omega, \tag{90}$$

to get the $1\sqrt{\omega}$ scaling. [11] Therefore, the upper cutoff is

$$\omega_u = \min(K^2, \sim 0.1) \tag{91}$$

if we allow a 10% error in approximation (90).

7.1. Numerical experiments

Fig. 7 is a time series obtained by numerically simulating the process in Eq. (80). The process λ_n is generated according to Eq. (81) with $\Delta = 1.25$ and $(\gamma - \alpha) = 1/128$. The additive noise ϵ_n is generated by an independent random number generator. It takes on values $\pm 10^{-6}$ at each time step. The range of x_n is restricted to $[-1, 1]$.

Fig. 8 shows the power spectrum for x_n^2 where x_n is the discrete-time on–off intermittent process in (80) with $\Delta = 4.0$, $\rho = 10^{-12}$ and $(\gamma - \alpha) = 1/1000$. The dashed line has the theoretical slope equal to $-\frac{1}{2}$. The analysis predicts a scaling range

$$5.7 \times 10^{-4} \ll \omega \ll 1.0 \times 10^{-1}, \tag{92}$$

and the data agrees well with the predicted slope and scaling range. With these values of the parameters, $K^2 > 0.1$ and so the upper cutoff is determined by the requirement that approximation (90) be valid.

Fig. 9 shows a numerically obtained plot to verify our scaling result of the number of boxes of rescaled length ϵ needed to cover the set of rescaled time indices where $|x_n|$ takes on values above a given threshold. The plot shows the number of boxes needed to cover the set of time indices where the process x_n in Eq. (80) with $\Delta = 1.25$, $\rho = 10^{-6}$ and $(\gamma - \alpha) = 1/128$ satisfies $|x_n| \geq 0.8$. The total number of samples is 2^{20} and we count the total number of boxes required for box sizes n in the range $2^3 < n < 2^{20}$. The rescaled length ϵ of each box is given by

$$\epsilon = (\gamma - \alpha)^2 n = 2^{-14} n. \tag{93}$$

We have plotted both $N(\epsilon)$ and ϵ on logarithmic scales.

---

[10] See Appendix B.
[11] See Appendix B Eq. (B.20).
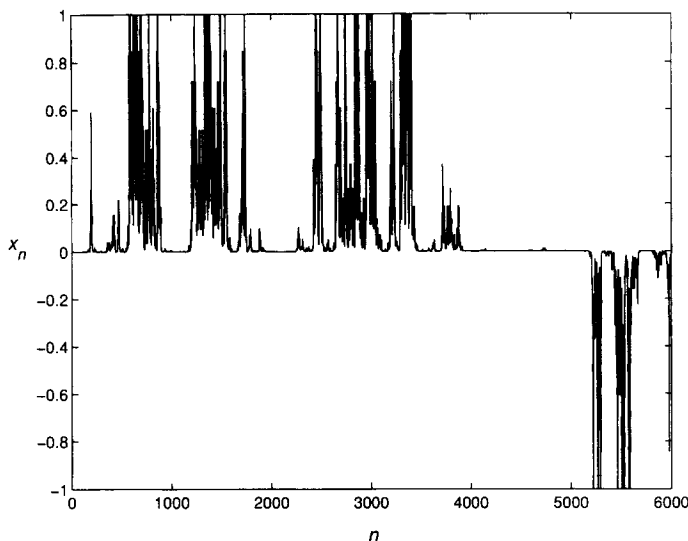
Fig. 7. Time series for a Discrete time on–off intermittent process with parameter values $\Delta = 1.25$, $\rho = 10^{-6}$ and $(\gamma - \alpha) = 1/128$.
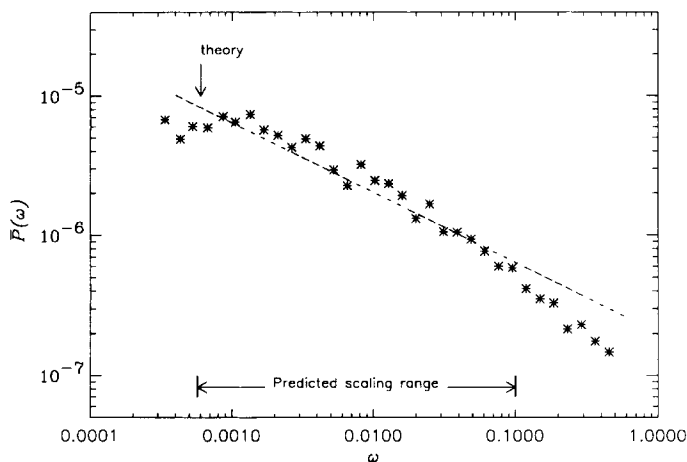
Fig. 8. Numerically obtained power spectrum for x_n^2 with $\Delta = 4.0$, $\rho = 10^{-12}$ and $(\gamma - \alpha) = 1/1000$. Both the axes are on log-scales.

The solid line has the theoretical slope of $-\frac{1}{2}$. From Fig. 9, we see that $N(\epsilon) \sim \epsilon^{-1/2}$ over a range of ϵ. Our analysis predicts that the range where $N(\epsilon) \sim \epsilon^{-1/2}$ is

$$6.1 \times 10^{-5} \ll \epsilon \ll 3.7 \times 10^{-2}. \tag{94}$$

The numerically obtained plot in Fig. 9 is consistent with this prediction.

8. Conclusions

In this paper we introduce a continuous-time model that displays on–off intermittency and models the universal properties of this kind of behavior near a blow-out bifurcation. Using this model, we derive scaling results
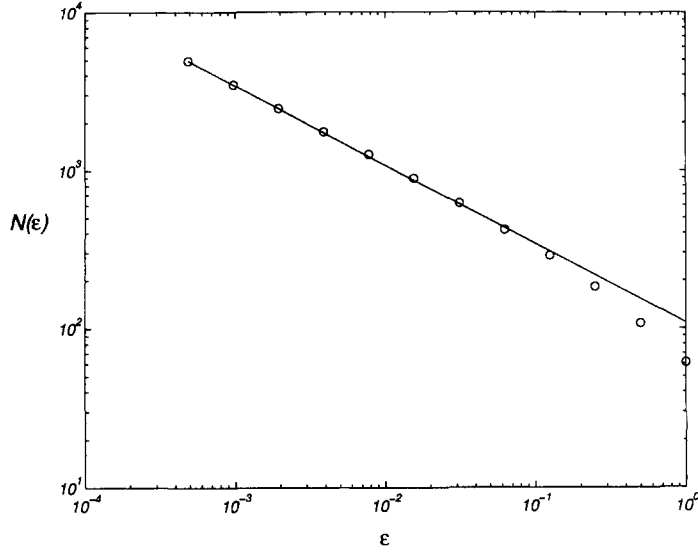
Fig. 9. A plot of $N(\epsilon)$ as a function of ϵ. The plot was obtained by numerically generating the process x_n with the parameter values $\Delta = 1.25$, $\rho = 10^{-6}$ and $(\gamma - \alpha) = 1/128$ and taking the set of time indices where $|x_n|$ is larger than or equal to 0.8. The solid line is the theoretical scaling result and it has a slope equal to $-\frac{1}{2}$.

(summarized in Section 3) for the power spectrum of the intermittent process and for the fractal dimension of the set of times when the process takes on values above a threshold both with and without additive noise. We compare our results to those reported in the literature. We also introduce a discrete-time model which displays on–off intermittency and incorporates the effects of additive noise. We numerically simulate this model and verify the universal scaling results we obtain from the continuous-time model.

Acknowledgements

Appendix A. On–off intermittency with noise

We consider a continuous-time on–off intermittent process with additive noise. The forward Kolmogorov equation for $p(x, t)$ is given by Eq. (30). We restrict the range of x by imposing no–flux boundary conditions at $x = 1$ and $x = -1$. Therefore,

$$\Gamma(x, t)|_{x=\pm 1} = 0 \quad \text{for all } t. \tag{A.1}$$

Define the linear operator $\mathcal{L}_x$ by

$$\mathcal{L}_x \psi(x) = a(x) \frac{\partial}{\partial x} [\psi(x)] + \frac{1}{2} b^2(x) \frac{\partial^2}{\partial x^2} [\psi(x)], \tag{A.2}$$

where $a(x)$ and $b(x)$ are the drift and the diffusion coefficients defined in Eq. (28). Then, Eq. (30) can be rewritten as

$$\frac{\partial p(x, t)}{\partial t} = \mathcal{L}_x^\dagger p(x, t), \tag{A.3}$$

where $\mathcal{L}_x^\dagger$ is the linear operator adjoint to $\mathcal{L}_x$. In the steady state,

$$\frac{\partial p(x, t)}{\partial t} = 0 \tag{A.4}$$

Therefore,

$$\mathcal{L}_x^\dagger p_{ss}(x) = 0. \tag{A.5}$$

We can solve for the steady state probability distribution of x to get

$$p_{ss}(x) = A(\beta^2 x^2 + \sigma^2)^{h/\beta^2 - 1/2}, \tag{A.6}$$

where A is a normalizing constant.

A.1. Power spectral density

As we discuss in Section 7, we calculate the power spectrum of $x^2(t)$ where $x(t)$ is the continuous-time on–off intermittent process in Eq. (25). The autocorrelation $R(\tau)$ is given by $E[x^2(t)x^2(t + \tau)]$ (see Eq. (73)). Therefore,

$$R(\tau) = \int_{-1}^{1} dx\, x^2 p_{ss}(x) \int_{-1}^{1} dy\, y^2 p_*(y, \tau : x), \tag{A.7}$$

where $p_*(y, \tau : x)$ is the transition probability density. The transition probability density satisfies the forward equation

$$\frac{\partial p*(y, \tau : x)}{\partial \tau} = \mathcal{L}_y^\dagger p_*(y, \tau : x) \tag{A.8}$$

with the initial condition

$$p_*(y, 0 : x) = \delta(x - y). \tag{A.9}$$

We can take the Laplace transform of the forwards equation to get

$$s\overline{p}(y, s : x) = \mathcal{L}_y^\dagger \overline{p}(y, s : x) + \delta(x - y). \tag{A.10}$$

Laplace transforming (A.7) gives

$$\overline{R}(s) = \int_{-1}^{1} dx\, x^2 p_{ss}(x) \int_{-1}^{1} dy\, y^2 \overline{p}(y, s : x), \tag{A.11}$$

where $\overline{R}(s)$ is the Laplace transform of the autocorrelation. Introduce the adjoint equation

$$s\chi(s, y) = \mathcal{L}_y \chi(s, y) + y^2. \tag{A.12}$$

Multiplying Eq. (A.12) by $\overline{p}(y, s : x)$ and integrating over y, we get

$$\int\limits_{-1}^{1} dy \, \overline{p}(y, s : x)(s\chi - \mathcal{L}_y \chi) = \int\limits_{-1}^{1} dy \, \overline{p}(y, s : x) y^2. \tag{A.13}$$

Integrating by parts gives

$$\int\limits_{-1}^{1} dy \, \overline{p} \mathcal{L}_y \chi = \int\limits_{-1}^{1} dy \, \chi \mathcal{L}_y^{\dagger} \overline{p} + \text{ boundary terms}, \tag{A.14}$$

and we obtain

$$\int\limits_{-1}^{1} dy \, \chi(s, y)(s\overline{p} - \mathcal{L}_y^{\dagger} \overline{p}) - \left[\frac{1}{2} b^2(x) \overline{p} \frac{\partial \chi}{\partial y} - \chi \overline{\Gamma}(y, s) \right]_{-1}^{1} = \int\limits_{-1}^{1} dy \, \overline{p}(y, s : x) y^2, \tag{A.15}$$

where $\overline{\Gamma}(y, s)$ is the Laplace transform of the flux. As we have no flux boundary conditions for p_*, if we impose the conditions

$$\frac{\partial \chi}{\partial y}\bigg|_{y=-1} = \frac{\partial \chi}{\partial y}\bigg|_{y=1} = 0, \tag{A.16}$$

and use Eq. (A.10), we have

$$\chi(x, s) = \int\limits_{-1}^{1} dy \, \overline{p}(y, s : x) y^2. \tag{A.17}$$

Therefore using Eq. (A.17) in Eq. (A.7) we obtain

$$\overline{R}(s) = \int\limits_{-1}^{1} dx \, \chi(x, s) x^2 p_{ss}(x). \tag{A.18}$$

$\chi(s, y)$ can be expressed in terms of hypergeometric functions. We introduce the variable

$$v = -\frac{\beta^2 y^2}{\sigma^2}, \tag{A.19}$$

and define the function $\psi(v, s)$ by

$$\psi(v, s) = \chi\left(\frac{\sigma}{\beta} \sqrt{-v}, s \right) \quad \text{for } 0 \geq v \geq -\frac{\beta^2}{\sigma^2}. \tag{A.20}$$

Then, rewriting Eq. (A.12) in v and $\psi(v, s)$ gives

$$v(1 - v) \frac{\partial^2 \psi(v, s)}{\partial v^2} + \left[\frac{1}{2} - \left(1 + \frac{h_\perp}{\beta^2} \right) v \right] \frac{\partial \psi(v, s)}{\partial v} + \frac{s}{2\beta^2} \psi(v, s) = -\frac{\sigma^2}{2\beta^4} v \tag{A.21}$$

with the boundary condition

$$\frac{\partial \psi(v, s)}{\partial v}\bigg|_{v=-\beta^2/\sigma^2} = 0. \tag{A.22}$$

The solution to the homogenous equation

$$x(1 - x)\frac{d^2 f}{dx^2} + [c - (1 + a + b)x]\frac{df}{dx} - abf = 0, \tag{A.23}$$

regular at the origin, is

$$f = F(a, b, c; x), \tag{A.24}$$

where

$$F(a, b, c; x) = 1 + \frac{ab}{1.c}x + \frac{a(a + 1)b(b + 1)}{1.2.c(c + 1)}x^2 + \cdots \tag{A.25}$$

is the hypergeometric function [24]. Therefore, the solution to Eq. (A.21) is

$$\psi(v, s) = A(s)F(\alpha_+, \alpha_-, 1/2; v) + \psi_0(v, s), \tag{A.26}$$

where

$$\alpha_\pm = \frac{h_\perp \pm \sqrt{h_\perp^2 + 2\beta^2 s}}{2\beta^2}. \tag{A.27}$$

$\psi_0(v, s)$ is a particular solution and $A(s)$ is chosen so as to satisfy the boundary condition. We can find a particular solution of Eq. (A.21) by assuming the form

$$\psi_0(v, s) = g_0(s) + vg_1(s). \tag{A.28}$$

We then obtain

$$\psi_0(v, s) = \frac{\sigma^2}{s - 2h_\perp - 2\beta^2}\left[\frac{1}{s} - \frac{v}{\beta^2}\right]. \tag{A.29}$$

Imposing the boundary condition (A.22) on (A.26) and using

$$\frac{d}{dx}F(a, b, c; x) = \frac{ab}{c}F(1 + a, 1 + b, 1 + c; x), \tag{A.30}$$

which is an identity [24], yields

$$A(s) = \frac{\sigma^2}{s(s - 2h_\perp - 2\beta^2)}\frac{1}{F(1 + \alpha_+, 1 + \alpha_-, 3/2; -\beta^2/\sigma^2)}. \tag{A.31}$$

Therefore, the complete solution of (A.21) and its associated boundary conditions is

$$\psi(v, s) = \frac{\sigma^2}{s - 2h_\perp - 2\beta^2}\left[\frac{1}{s}\left(1 - \frac{F(\alpha_+, \alpha_-, 1/2; v)}{F(1 + \alpha_+, 1 + \alpha_-, 3/2; -\beta^2/\sigma^2)}\right) - \frac{v}{\beta^2}\right]. \tag{A.32}$$

It would appear that $\psi(v, s)$ has a pole in the right half-plane at $s = 2h_\perp + 2\beta^2$. However, setting $s = 2h_\perp + 2\beta^2$ in (A.27) gives $\alpha_- = -1$. The hypergeometric functions have the properties,

$$F(a, -1, c; x) = 1 - \frac{a}{c}x,$$

$$F(a, 0, c; x) = 1 \tag{A.33}$$
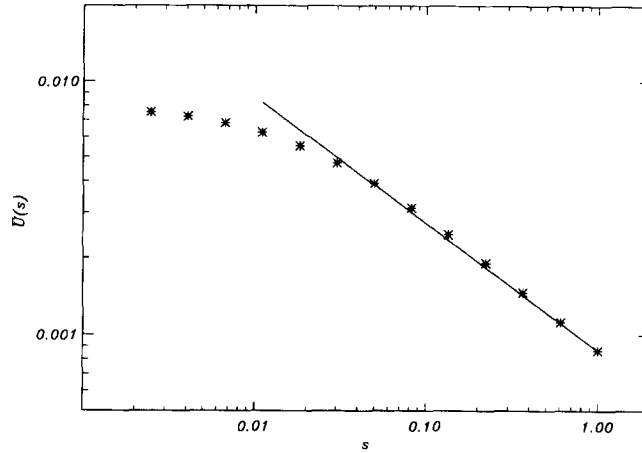
Fig. 10. $\overline{U}(s)$ as a function of s for real s. The parameters have values $\beta = 1$, $h_\perp = 10^{-3}$ and $\sigma = 10^{-6}$. The solid line has a slope equal to $-\frac{1}{2}$.

(see (A.25), [24]). Thus at $s = 2h_\perp + 2\beta^2$, we have

$$F(\alpha_+, \alpha_-, 1/2; v) = 1 - 2\alpha_+ v,$$
$$F(1 + \alpha_+, 1 + \alpha_-, 3/2; v) = 1. \tag{A.34}$$

Therefore,

$$\frac{1}{s}\left(1 - \frac{F(\alpha_+, \alpha_-, 1/2; v)}{F(1 + \alpha_+, 1 + \alpha_-, 3/2; -\beta^2/\sigma^2)}\right) - \frac{v}{\beta^2} = 0 \tag{A.35}$$

at $s = 2h_\perp + 2\beta^2$, and so we do not have a pole in the right half-plane. We can now get an expression for $\chi(x, s)$ from (A.20) and (A.32)

$$\chi(x, s) = \frac{\sigma^2}{s - 2h_\perp - 2\beta^2}\left[\frac{1}{s}\left(1 - \frac{F(\alpha_+, \alpha_-, 1/2; -\beta^2 x^2/\sigma^2)}{F(1 + \alpha_+, 1 + \alpha_-, 3/2; -\beta^2/\sigma^2)}\right) + \frac{x^2}{\sigma^2}\right]. \tag{A.36}$$

Eq. (A.18) gives an expression for $\overline{R}(s)$ which can now be evaluated using the expression for $\chi(x, s)$ in (A.36). As we discussed in Section 5.1, $\overline{R}(s)$ has a pole at $s = 0$. Therefore, we use Eq. (49) for $\overline{U}(s)$, the Laplace transform of the autocovariance. This function does not have any singularities in the right-half s-plane or the imaginary axis.

Fig. 10 shows a log-log plot of $\overline{U}(s)$ as a function of s (for real s) for $\beta = 1$, $h_\perp = 10^{-3}$ and $\sigma = 10^{-6}$. It was obtained by numerically integrating (A.18) for $\overline{R}(s)$ and removing the contribution of the pole at $s = 0$. From the figure, we see that there is a corner frequency ω_c such that $\overline{U}(s)$ is a contant for $s < \omega_c$ and $\overline{U}(s) \sim 1/\sqrt{s}$ for $s > \omega_c$.

The hypergeometric functions satisfy

$$F(a, b, c, x) = (1 - x)^{-b} F(b, c - a, c, -x/(1 - x)). \tag{A.37}$$

as an identity [24]. Furthermore,

$$F(a, b, c, 1) = \frac{\Gamma(c)\Gamma(c - a - b)}{\Gamma(c - a)\Gamma(c - b)} \tag{A.38}$$

if $Real(c - a - b) > 0$ [24]. Therefore, if $|v| \gg 1$, $v < 0$ and $Real(a - b) > 0$,

$$F(a, b, c, v) \approx (1 - v)^{-b} \frac{\Gamma(c)\Gamma(a - b)}{\Gamma(a)\Gamma(c - b)} \tag{A.39}$$

with corrections of the order $1/v^{b+1}$. For $s \gg h_\perp^2/D$, we have $\alpha_\pm = \pm\sqrt{s/2\beta^2}$.

$$F(a, -a, 1/2, -z^2) = \cosh(2a \log((1 + z^2)^{1/2} + z)) \tag{A.40}$$

is an identity [24]. Using approximation (A.39) for $F(a, -a, 1/2, -z^2)$ gives

$$F(a, -a, 1/2, -z^2) \sim (1 + z^2)^a. \tag{A.41}$$

Comparison with Eq. (A.40) shows that this is valid only when $2a \log((1 + z^2)^{1/2} + z) \gg 1$. As $z \approx \beta/\sigma$, we require that

$$s \gg 2\beta^2 \left[\log\left(\frac{\beta^2}{\sigma^2}\right)\right]^{-2}. \tag{A.42}$$

Using approximation (A.39) in (A.36) with $s \ll 2\beta^2$ and $h_\perp \ll 2\beta^2$, we obtain

$$\chi(x, s) \approx \frac{\sigma^2}{2\beta^2}\left[\frac{1}{s}\left(2\alpha + \frac{(1 + \beta^2 x^2/\sigma^2)^{-\alpha^-}}{(1 + \beta^2/\sigma^2)^{-1-\alpha_-}} - 1\right) + \frac{x^2}{\sigma^2}\right]. \tag{A.43}$$

Substituting in Eq. (A.18) and expanding in powers of σ/β yields

$$\overline{R}(s) = \frac{A\beta^{(2h_\perp/\beta^2-1)}}{2h_\perp/\beta^2 + 1 - \alpha_-}\left[\frac{\alpha_+}{s} + O\left(\frac{\sigma^2}{\beta^2}\right)\right]. \tag{A.44}$$

Therefore, $\overline{R}(s) \sim 1/\sqrt{s}$ in the range where all the approximations are valid. In this range, $\overline{P}(\omega) = \overline{R}(i\omega) + \overline{R}(-i\omega)$ implies that the power spectrum scales as $1/\sqrt{\omega}$. From the above discussion and Eq. (A.42) we see that the scaling range for the power spectrum is given by Eq. (13). This proves the first part of our results in item (iii) of Section 3.

A.2. Fractal dimension

We want to evaluate $P(\epsilon)$, the probability of being absorbed in a time interval of rescaled length ϵ at $x = \pm1$. To evaluate this probability we consider the transition probability density $p_*(y, t : x)$ which satisfies the Backward Kolmogorov [12] equation [23]

$$\frac{\partial p_*(y, t : x)}{\partial t} = \mathcal{L}_x p_*(y, t : x), \tag{A.45}$$

with absorbing boundary conditions at $x = \pm1$,

$$p_*(y, t : -1) = p_*(y, t : 1) = 0, \tag{A.46}$$

and the initial condition

$$p_*(y, 0 : x) = \delta(y - x) \quad \text{for } x \in (-1, 1), \tag{A.47}$$

---

[12] This is a differential equation for the transition probability density $p(y, t : x)$ in the "backward" variable x.

which is true for all transition probability densities. We define a function $q(x, t)$ by

$$q(x, t) = \int_{-1}^{1} dy \, p_*(y, t : x). \tag{A.48}$$

Then, $q(x_0, t)$ is the probability of not being absorbed in a time t if we start out at $x = x_0$. Eq. (A.45) gives

$$\frac{\partial q(x, t)}{\partial t} = \mathcal{L}_x q(x, t). \tag{A.49}$$

The absorbing boundary conditions give

$$q(-1, t) = q(1, t) = 0, \tag{A.50}$$

and the initial condition implies

$$q(x, 0) = 1 \quad \text{for } x \in (-1, 1). \tag{A.51}$$

Taking the Laplace transform of Eq. (A.49) we obtain

$$(\mathcal{L}_x - s)\overline{q}(x, s) = -1 \tag{A.52}$$

with boundary conditions

$$\overline{q}(-1, s) = \overline{q}(1, s) = 0. \tag{A.53}$$

It is again convenient to introduce the variable v by

$$v = -\frac{\beta^2}{\sigma^2} x^2, \tag{A.54}$$

and define the function $\phi(v, s)$ by

$$\phi(v, s) = \overline{q}\left(\frac{\sigma}{\beta}\sqrt{-v}, s\right) \quad \text{for } 0 \geq v \geq -\frac{\beta^2}{\sigma^2}. \tag{A.55}$$

Expressing Eq. (A.52) and its associated boundary condition in terms of the new variables gives

$$v(1 - v)\frac{\partial^2 \phi(v, s)}{\partial v^2} + \left[\frac{1}{2} - \left(1 + \frac{h}{\beta^2}\right)v\right]\frac{\partial \phi(v, s)}{\partial v} + \frac{s}{2\beta^2}\phi(v, s) = \frac{1}{2\beta^2} \tag{A.56}$$

with the boundary condition

$$\phi\left(-\frac{\beta^2}{\sigma^2}, s\right) = 0. \tag{A.57}$$

The solution to Eq. (A.56) is

$$\phi(v, s) = B(s)F(\alpha_+, \alpha_-, 1/2; v) + \phi_0(v, s), \tag{A.58}$$

where $\alpha_\pm$ is given by Eq. (A.27). $\phi_0(v, s)$ is a particular solution and $B(s)$ is chosen so as to satisfy the boundary condition. A particular solution of Eq. (A.56) is

$$\phi_0(v, s) = \frac{1}{s}. \tag{A.59}$$

Imposing the boundary condition on the solution yields

$$B(s) = -\frac{1}{s F(\alpha_+, \alpha_-, 1/2; -\beta^2/\sigma^2)}.$$ (A.60)

Therefore,

$$\phi(v, s) = \frac{1}{s}\left[1 - \frac{F(\alpha_+, \alpha_-, 1/2; v)}{F(\alpha_+, \alpha_-, 1/2; -\beta^2/\sigma^2)}\right],$$ (A.61)

and using the definition of ϕ, we have

$$\bar{q}(x, s) = \frac{1}{s}\left[1 - \frac{F(\alpha_+, \alpha_-, 1/2; -\beta^2 x^2/\sigma^2)}{F(\alpha_+, \alpha_-, 1/2; -\beta^2/\sigma^2)}\right].$$ (A.62)

We start of with an initial probability distribution $p_0(x) = p_{ss}(x)$. The probability $W(t)$ of being absorbed in a (unscaled) time t is given by

$$W(t) = 1 - \int_{-1}^{1} dx\, p_{ss}(x) q(x, t).$$ (A.63)

Therefore,

$$\frac{dW(t)}{dt} = -\int_{-1}^{1} dx\, p_{ss}(x) \frac{\partial q(x, t)}{\partial t}.$$ (A.64)

Using Eq. (A.49), we have

$$\frac{dW(t)}{dt} = -\int_{-1}^{1} dx\, p_{ss}(x) \mathcal{L}_x(q(x, t)).$$ (A.65)

Integrating by parts gives

$$\frac{dW(t)}{dt} = -\int_{-1}^{1} dx\, q(x, t) \mathcal{L}_x^\dagger p_{ss}(x) + \left[q(x, t)\Gamma_{ss}(x) - \frac{1}{2}b^2(x)p_{ss}(x)\frac{\partial q(x, t)}{\partial x}\right]_{-1}^{1},$$ (A.66)

where

$$\Gamma_{ss}(x) = -\frac{1}{2}\frac{\partial}{\partial x}\left[b^2(x)p_{ss}(x)\right] + a(x)p_{ss}(x)$$ (A.67)

is the probability flux in the steady state. Therefore, $\Gamma_{ss}(x) = 0$. Also, by Eq. (A.5),

$$\mathcal{L}_x^\dagger p_{ss}(x) = 0.$$ (A.68)

So we get

$$\frac{dW(t)}{dt} = -\frac{1}{2}b^2(x)p_{ss}(x)\frac{\partial q(x, t)}{\partial x}\Big|_{-1}^{1}.$$ (A.69)
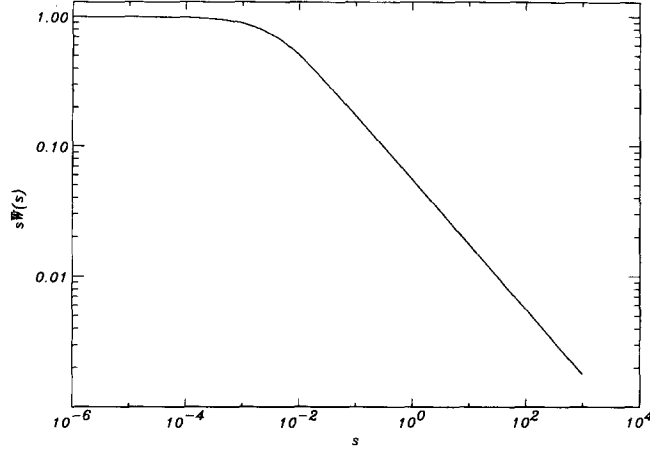
Fig. 11. $s\overline{W}(s)$ vs. s. The parameters have values $\beta = 1$, $h_\perp = 10^{-2}$ and $\sigma = 10^{-6}$.

Let $\overline{W}(s)$ be the Laplace transform of $W(t)$. Laplace transforming the previous equation yields

$$s\overline{W}(s) = w(0) + \left[-\frac{1}{2}b^2(x)p_{\rm ss}(x)\frac{\partial \overline{q}(x,s)}{\partial x} \right]_{-1}^{1}. \tag{A.70}$$

Eq. (A.62) along with the identity (A.30) and $w(0) = 0$ gives

$$\overline{W}(s) = \frac{1}{s}\frac{2p_{\rm ss}(1)(\beta^2 + \sigma^2)}{\sigma^2}\frac{F(1+\alpha_+, 1+\sigma_-, 3/2; -\beta^2/\sigma^2)}{F(\alpha_+, \alpha_-, 1/2; -\beta^2/\sigma^2)}. \tag{A.71}$$

With absorbing boundary conditions at $x = \pm 1$, the probability of eventually getting absorbed is unity independent of the initial distribution. Therefore, $W(t) \to 1$ when $t \to \infty$. This implies

$$\lim_{s\to 0} s\overline{W}(s) = 1. \tag{A.72}$$

Using

$$\lim_{s\to 0} \frac{F(1+\alpha_+, 1+\alpha_-, 3/2; -\beta^2/\sigma^2)}{F(\alpha_+, \alpha_-, 1/2; -\beta^2/\sigma^2)} = \frac{F(1+h/\beta^2, 1, 3/2; -\beta^2/\sigma^2)}{F(h/\beta^2, 0, 1/2; -\beta^2/\sigma^2)}, \tag{A.73}$$

we can evaluate the constant $p_{\rm ss}(1)$. Therefore,

$$\overline{W}(s) = \frac{1}{s}\left[\frac{F(h/\beta^2, 0, 1/2; -\beta^2/\sigma^2)}{F(1+h/\beta^2, 1, 3/2; -\beta^2/\sigma^2)} \frac{F(1+\alpha_+, 1+\alpha_-, 3/2; -\beta^2/\sigma^2)}{F(\alpha_+, \alpha_-, 1/2; -\beta^2/\sigma^2)} \right]. \tag{A.74}$$

Fig. 11 shows a log–log plot of $s\overline{W}(s)$ as a function of s (for real s) with parameter values $\beta = 1$, $h_\perp = 10^{-2}$ and $\sigma = 10^{-6}$. We see that there is a corner frequency ω_c such that $s\overline{W}(s) = 1$ for $s < \omega_c$ and $s\overline{W}(s) \sim 1/\sqrt{s}$ for $s > \omega_c$. We evaluate ω_c by obtaining the asymptotes of $\overline{W}(s)$ and finding their point of intersection.

For low frequencies, i.e., in the limit $s \to 0$, Eq. (A.74) yields

$$\overline{W}(s) = \frac{1}{s}, \tag{A.75}$$

as the equation of the low-frequency asymptote. Taking a Taylor series expansion, we get

$$\frac{F[h_\perp/\beta^2, 0, 1/2, -\beta^2/\sigma^2]}{F[1+h_\perp/\beta^2, 1, 3/2, -\beta^2/\sigma^2]} = \frac{F[0, 0, 1/2, -\beta^2/\sigma^2]}{F[1, 1, 3/2, -\beta^2/\sigma^2]} + {\rm O}(h_\perp). \tag{A.76}$$

Using the approximation (A.39), we have

$$\frac{F(1+\alpha_+, 1+\alpha_-, 3/2; -\beta^2/\sigma^2)}{F(\alpha_+, \alpha_-, 1/2; -\beta^2/\sigma^2)} \approx \frac{\sigma^2}{2\alpha_+(\sigma^2+\beta^2)}. \tag{A.77}$$

We also have [24]

$$\frac{F[0, 0, 1/2, -\beta^2/\sigma^2]}{F[1, 1, 3/2, -\beta^2/\sigma^2]} = \frac{\sigma^2 \sinh^{-1}(\beta/\sigma)}{\beta(\beta^2+\sigma^2)^{1/2}}. \tag{A.78}$$

If $\beta/\sigma \gg 1$, we get

$$\sinh^{-1}(\beta/\sigma) \approx \log(2\beta/\sigma). \tag{A.79}$$

We obtain the equation of the high-frequency asymptote for $\overline{W}(s)$ by substituting from the above equations in (A.74). This yields

$$\overline{W}(s) = \frac{\sqrt{2\beta^2}}{\log(4\beta^2/\sigma^2)s^{3/2}} \tag{A.80}$$

as the equation of the high frequency asymptote. Therefore $\overline{W}(s) \sim s^{-3/2}$ for $s \gg \omega_c$, so that $W(t) \sim t^{1/2}$ for $t \ll w_c^{-1}$. From Eqs. (A.75) and (A.80), we obtain the expression for the corner frequency in Eq. (76). From the discussion in Sections 4 and 5.2, we expect the results we derive to be universal only for $\epsilon \gg h_\perp^2/D^2$. Therefore,

$$P(\epsilon) = W(D\epsilon/h_\perp^2) \sim \epsilon^{1/2} \tag{A.81}$$

for

$$h_\perp^2/D^2 \ll \epsilon \ll h_\perp^2/D\omega_c. \tag{A.82}$$

Appendix B. Noise free discrete-time model

We consider the process

$$x_{n+1} = \lambda_n x_n. \tag{B.1}$$

The process λ_n is generated by i.i.d random variables that take on a value $1/\Delta$ with a probability α and a value Δ with a probability $\gamma = 1 - \alpha$, where $\Delta \geq 1$. The average Lyapunov exponent is denoted by $\overline{h}$ and is given by Eq. (82). If we define the process u_n by $u_n = -\log(x_n)/\log(\Delta)$, we have

$$u_{n+1} = \begin{cases} u_n + 1 & \text{with probability } \alpha, \\ u_n - 1 & \text{with probability } \gamma. \end{cases} \tag{B.2}$$

If we choose x_0 to be Δ^{-m} for some integer m, $u_0 = m$ and the process u_n is a random walk on the lattice of integers. We restrict the range of x_n to [0,1] by replacing (B.2) by

$$u_{n+1} = \begin{cases} 1 & \text{with probability } \alpha, \\ 0 & \text{with probability } \gamma \end{cases} \tag{B.3}$$

if $u_n = 0$. The process that is defined by Eq. (B.2) for $u_n \geq 1$ and Eq. (B.3) for $u_n = 0$ is a random walk on the integer lattice with a reflecting boundary at 0. Then, $x_n = e^{-Ku_n}$ is a discrete-time on–off intermittent process where $K = \log(\Delta)$.

B.1. Power spectral density

The autocorrelation r_n for the process x_n is given by Eq. (86). From this we have,

$$r_n = E[\mathrm{e}^{-Ku_p}\mathrm{e}^{-Ku_{n+p}}]. \tag{B.4}$$

Let $p(l, n : m)$ be the transition probability, i.e., the probability that $u_{n+q} = l$ given that $u_q = m$. If $p_{ss}(m)$ is the probability that $u_n = m$ in the steady state, we have

$$r_n = \sum_{l=0}^{\infty} \sum_{m=0}^{\infty} p_{ss}(m)\mathrm{e}^{-Km} p(l, n : m)\mathrm{e}^{-Kl}. \tag{B.5}$$

The transition probability satisfies the equations

$$
\begin{aligned}
p(l, n + 1 : m) &= \alpha p(l - 1, n : m) + \gamma p(l + 1, n : m) \quad \text{for } l \geq 1, \\
p(0, n + 1 : m) &= \gamma p(0, n : m) + \gamma p(l, n : m).
\end{aligned} \tag{B.6}
$$

In the steady state,

$$p_{ss}(l) = \alpha p_{ss}(l - 1) + \gamma p_{ss}(l + 1) \quad \text{for } l \geq 1, \tag{B.7}$$

$$p_{ss}(0) = \gamma p_{ss}(0) + \gamma p_{ss}(1). \tag{B.8}$$

These equations along with the condition

$$\sum_{l=0}^{\infty} p_{ss}(l) = 1$$

yield

$$p_{ss}(l) = \frac{\gamma - \alpha}{\gamma} \left(\frac{\alpha}{\gamma}\right)^l. \tag{B.9}$$

Let

$$\tilde{p}(l, z : m) = \sum_{n=0}^{\infty} p(l, n : m) z^{-n} \tag{B.10}$$

be the $\mathcal{Z}$-transform of $p(l, n : m)$ with respect to n. Then, Eq. (B.6) gives

$$
\begin{aligned}
z[\tilde{p}(l, z : m) - p(l, 0 : m)] &= \alpha \tilde{p}(l - 1, z : m) + \gamma \tilde{p}(l + 1, z : m) \quad \text{for } l \geq 1, \\
z[\tilde{p}(0, z : m) - p(0, 0 : m)] &= \gamma \tilde{p}(0, z : m) + \gamma \tilde{p}(1, z : m).
\end{aligned} \tag{B.11}
$$

Define

$$
\begin{aligned}
\eta &= \frac{\alpha}{\gamma}, \qquad \mu = \mathrm{e}^{-K}, \qquad \Gamma = \alpha\mu + \frac{\gamma}{\mu}, \\
\xi &= \frac{z - \sqrt{z^2 - 4\alpha\gamma}}{2\gamma}, \\
\overline{p}(l, z) &= \sum_{m=0}^{\infty} \tilde{p}(l, z : m) p_{ss}(m)\mathrm{e}^{-Km}.
\end{aligned} \tag{B.12}
$$

Using the initial condition on the transition probability

$$p(l, 0 : m) = \delta_{lm},$$
(B.13)

and Eq. (B.11), we have

$$z[\overline{p}(l, z) - (1 - \eta)(\eta\mu)^l] = \alpha\overline{p}(l - 1, z) + \gamma\overline{p}(l + 1, z) \quad \text{for } l \geq 1,$$

$$z[\overline{p}(0, z) - (1 - \eta)] = \gamma\overline{p}(0, z) + \gamma\overline{p}(1, z).$$
(B.14)

We can solve Eq. (B.14) imposing the boundary condition $\overline{p}(l, z) \to 0$ as $l \to \infty$ to obtain

$$\overline{p}(l, z) = A\xi^l + B(\eta\mu)^l,$$
(B.15)

where

$$A = \frac{(1 - \eta)(1 - \xi)}{1 - \eta\mu}\left[\frac{z}{z - 1} - \frac{z}{z - \Gamma}\right],$$

$$B = (1 - \eta)\left[\frac{z}{z - \Gamma}\right].$$
(B.16)

Using Eq. (B.5) we have

$$C(z) = \sum_{l=0}^{\infty} \overline{p}(l, z)\mu^l,$$
(B.17)

where $C(z) = \sum_{n=0}^{\infty} r_n z^{-n}$ is the $\mathcal{Z}$-transform of the autocorrelation r_n. Therefore,

$$C(z) = \frac{A}{1 - \xi\mu} + \frac{B}{1 - \eta\mu^2}.$$
(B.18)

The power spectral density $\tilde{P}(e^{i\omega})$ is given by Eq. (88). Therefore, using the definition of p_n in Eq. (87), we get

$$\tilde{P}(e^{i\omega}) = C(e^{i\omega}) + C(e^{i\omega}) + p_0 - 2r_0.$$
(B.19)

In the limit $(\gamma - \alpha) \to 0$, and using $e^{i\omega} - 1 \approx i\omega$, we get

$$\tilde{P}(e^{i\omega}) = \frac{1}{K^2}\sqrt{\frac{8}{\omega}}$$
(B.20)

for $(\gamma - \alpha)^2 \ll \omega \ll \min(K^2, 1)$, which is our scaling result.

B.2. Fractal dimension

We calculate the fractal dimension of the set $\mathcal{N}$ of times when the process takes on values above a given threshold. $\mathcal{N} = \{n \mid x_n = 1\} = \{n \mid u_n = 0\}$. Consider the random walk in Eq. (B.2) with an absorbing boundary at $z = 0$. Then we have

$$u_{n+1} = \begin{cases} u_n + 1 & \text{with probability } \alpha, \\ u_n - 1 & \text{with probability } \gamma \end{cases}$$
(B.21)

if $u_n \geq 1$, and

$$u_{n+1} = 0$$
(B.22)

if $u_n = 0$. If $p(l, n)$ is the probability that $u_n = l$, we have

$$p(l, n + 1) = \alpha p(l - 1, n) + \gamma p(l + 1, n) \quad \text{for } l \geq 2,$$
$$p(1, n + 1) = \gamma p(2, n),$$
$$p(0, n + 1) = p(0, n) + \gamma p(1, n). \tag{B.23}$$

We impose the initial condition

$$p(l, 0) = p_{ss}(l). \tag{B.24}$$

Let $\overline{p}(l, z)$ denote the $\mathcal{Z}$-transform of $p(l, n)$ with respect to the variable n. Then,

$$\overline{p}(l, z) = \sum_{n=0}^{\infty} p(l, n) z^{-n}. \tag{B.25}$$

Eq. (B.23) yields

$$z[\overline{p}(l, z) - p_{ss}(l)] = \alpha \overline{p}(l - 1, z) + \gamma \overline{p}(l + 1, z) \quad \text{for } l \geq 2,$$
$$z[\overline{p}(1, z) - p_{ss}(1)] = \gamma \overline{p}(2, z),$$
$$z[\overline{p}(0, z) - p_{ss}(0)] = \overline{p}(0, z) + \gamma \overline{p}(1, z). \tag{B.26}$$

Let $W(z) = \overline{p}(0, z)$. We can solve for $W(z)$ to obtain

$$\frac{W(z)}{(\gamma - \alpha)} = \left(\frac{\gamma}{\alpha}\right) \frac{1 - \sqrt{1 - 4\alpha\gamma z^{-2}}}{2\gamma z^{-1} - 1 + \sqrt{1 - 4\alpha\gamma z^{-2}}}. \tag{B.27}$$

Expanding about $(\gamma - \alpha) = 0$, we have

$$\frac{W(z)}{(\gamma - \alpha)} = \frac{1}{1 - z^{-1}} \left[\sqrt{\frac{1 + z^{-1}}{1 - z^{-1}}} - 1 \right] + \mathrm{O}((\gamma - \alpha)). \tag{B.28}$$

The probability of being absorbed in n steps, $w(n)$, is the inverse $\mathcal{Z}$-transform of $W(z)$. Therefore, we have

$$w(n) = (\gamma - \alpha)(\sqrt{n} + \mathrm{O}(1)) + \mathrm{O}((\gamma - \alpha)^2 n). \tag{B.29}$$

For $n \gg 1$ and $(\gamma - \alpha)^2 n \ll 1$, we have

$$p(\epsilon) = w(n) = \sqrt{(\gamma - \alpha)^2 n}. \tag{B.30}$$

Using Eq. (53) and the fact that $\epsilon = (\gamma - \alpha)^2 n$, we have the scaling result

$$N(\epsilon) = \epsilon^{-1/2} \quad \text{for } (\gamma - \alpha)^2 \ll \epsilon \ll 1. \tag{B.31}$$

References

[1] E. Ott and J.C. Sommerer, Phys. Lett. A 188 (1994) 39.
[2] N. Platt, E.A. Spiegel and C. Tresser, Phys. Rev. Lett. 70 (1993) 279.
[3] P. Ashwin, J. Buescu and I.N. Stewart, Phys. Lett. A 193 (1994) 126.
[4] P.W. Hammer, N. Platt, S.M. Hammel, J.F. Heagy and B.D. Lee, Phys. Rev. Lett. 73 (1994) 1095.
[5] P. Ashwin, J. Buescu and I.N. Stewart, From Attractor to Chaotic Saddle: a tale of transverse instability, preprint (1994).

[6] H. Fujisaka, H. Ishii, M. Inoue and T. Yamada, Prog. Theor. Phys. 76 (1986) 1198.
[7] A.S. Pikovsky, Z. Phys. B 55 (1984) 149.
[8] A.S. Pikovsky and P. Grassberger, J. Phys. A 24 (1991) 4587.
[9] A.S. Pikovsky, Phys. Lett. A 165 (1992) 33.
[10] H. Fujisaka and T. Yamada, Prog. Theor. Phys. 74 (1985) 919.
[11] H. Fujisaka and T. Yamada, Prog. Theor. Phys. 75 (1986) 1087.
[12] L. Yu, E. Ott and Q. Chen, Phys. Rev. Lett. 65 (1990) 2935.
[13] L. Yu, E. Ott and Q. Chen, Physica D 53 (1992) 102.
[14] J.F. Heagy, N. Platt and S.M. Hammel, Phys. Rev. E 49 (1994) 1140.
[15] N. Platt, S. M. Hammel and J.F. Heagy, Phys. Rev. Lett. 72 (1994) 3498.
[16] M. Ding and W. Wang, Distribution of First Return Time in Fractional Brownian Motion and its Application to the Study of On–Off Intermittency, preprint.
[17] Y. Pomeau and P. Manneville, Commun. Math. Phys. 74 (1980) 189.
[18] E. Stone and P. Holmes, SIAM J. Appl. Math. 50 (1990) 726.
[19] E. Stone and P. Holmes, Phys. Lett. A 155 (1991) 29.
[20] E. Ott, J.C. Alexander, I. Kan, J.C. Sommerer and J.A. Yorke, Physica D 76 (1994) 384.
[21] V.I. Oseledec, Trans. Mosc. Math. Soc. 19 (1968) 197.
[22] P. Walters, An Introduction to Ergodic Theory (Springer, New York, 1982).
[23] Z. Schuss, Theory and Applications of Stochastic Differential Equations (Wiley, New York, 1980).
[24] M. Abramowitz and I. A. Stegun, Handbook of mathematical functions (Dover, New York, 1965).
[25] A.V. Oppenheim and R.W. Schafer, Digital Signal Processing (Prentice-Hall, Engelwood Cliffs, NJ, 1989).